Numerical simulations of the Macondo well blowout reveal strong control of oil flow by reservoir permeability and exsolution of gas

Curtis M. Oldenburg[1], Barry M. Freifeld, Karsten Pruess,
Lehua Pan, Stefan Finsterle, and George J. Moridis

Earth Sciences Division, MS 90-1116
1 Cyclotron Rd.
Lawrence Berkeley National Laboratory
Berkeley, CA 94720

[1]corresponding author
cmoldenburg@lbl.gov
510-486-7419
510-486-5686 (fax)

June 27, 2011

Abstract

In response to the urgent need for estimates of the oil and gas flow rate from the Macondo well MC252-1 blowout, we assembled a small team and carried out oil and gas flow simulations using the TOUGH2 codes over two weeks in mid-2010. The conceptual model included the oil reservoir and the well with a top boundary condition located at the bottom of the blowout preventer. We developed a fluid properties module (Eoil) applicable to a simple two-phase and two-component oil-gas system. The flow of oil and gas was simulated using T2Well, a coupled reservoir-wellbore flow model, along with iTOUGH2 for sensitivity analysis and uncertainty quantification. The most likely oil flow rate estimated from simulations based on the data available in early June 2010 was about 100,000 bbl/d (barrels per day) with a corresponding gas flow rate of 300 MMscf/d (million standard cubic feet per day) assuming the well was open to the reservoir over 30 m of thickness. A Monte Carlo analysis of reservoir and fluid properties provided an uncertainty distribution with a long tail extending down to 60,000 bbl/d of oil (170 MMscf/d of gas). The flow rate was most strongly sensitive to reservoir permeability. Conceptual model uncertainty was also significant, particularly with regard to the length of the well that was open to the reservoir. For fluid-entry interval length of 1.5 m, the oil flow rate was about 56,000 bbl/d. Sensitivity analyses showed that flow rate was not very sensitive to pressure-drop across the blowout preventer due to the interplay between gas exsolution and oil flow rate.

Introduction

On April 20, 2010, the Macondo well MC252-1 drilled from the Deepwater Horizon floating platform in the Gulf of Mexico suffered a blowout. Eleven people were killed by the explosion and fire on the platform shortly after the blowout, and the platform sank two days later. The failure of the blowout preventer (BOP) mounted on the wellhead at the seafloor allowed oil and gas to flow directly into the sea out of the mangled riser pipe, which would normally convey oil from the well to the platform. Later the riser pipe was cut off, and oil and gas flowed directly into the sea out the top of the BOP. These details were displayed to the public in unprecedented fashion in real time over the internet by live video feeds from several remotely operated vehicles.

Attention was focused in the first days and weeks after the blowout on devising strategies to stop the flow of oil. But as various strategies to stop the uncontrolled release were attempted and abandoned as unsuccessful, interest grew in estimating the magnitude of the oil and gas discharge into the marine environment. This information would be critical for addressing the environmental consequences of the oil and gas release, for developing engineering solutions for a temporary containment cap, and for evaluating the liability of the operating companies for environmental damage.

The Flow Rate Technical Group (FRTG) was established by the National Incident Commander (Admiral Thad Allen) on May 19, 2010, to estimate the oil flow rate. One component of the FRTG effort was assigned to a subgroup called the Nodal Team comprising investigators from the U.S. Department of Energy National Laboratories (NETL,

LLNL, LANL, PNNL, and LBNL), who were charged with making an independent estimate of the oil flow rate based on the physical properties and behavior of the reservoir fluids, wellbore, and seafloor attachments such as the BOP and riser pipe as constrained by the limited data at hand, such as reservoir pressure, temperature, and fluid composition, along with various assumptions about flow pathways through the well, annulus, BOP, and riser pipe. The approach used was numerical simulation of the flow of oil and gas from the reservoir, up the well, and into the marine environment based on the physics of two-phase flow in permeable media and the well, as opposed to direct measurements based on seafloor, sea surface, or aerial observations.

In this paper, we describe the work carried out by the LBNL team during the two weeks from the end of May to the middle of June 2010. Our work utilized various LBNL modeling tools, some of which we have been developing and using for more than 20 years for applications such as subsurface contamination by non-aqueous liquids (NAPLs), geothermal energy production, geologic carbon dioxide sequestration, nuclear waste disposal, and environmental hydrology. Despite the fact that we have not previously worked in the area of estimating oil flow in wells, our experience with multiphase flow and the LBNL computational tools facilitated relatively easy adaptations applicable to this urgent need for an oil flow-rate estimate.

While the charge to the Nodal Team was to estimate the oil flow rate, the natural (solution) gas component was known to make up a large part of the fluid leaking out of the BOP and was included as a fundamental part of our conceptual model. The behavior of the oil-gas system, which changes from single-phase liquid oil at the high pressures of the deep oil reservoir, to a two-phase oil-gas mixture in the well and at the seafloor as the pressure decreases, turned out to play an important role in controlling oil flow rate, as we will describe below. Although largely ignored during the early period of hydrocarbon release to the sea, the gas component was a large fraction of the total hydrocarbons that entered the ecosystem.

Because we had the capability of coupling the flow in the reservoir to that in the wellbore, and of discerning the individual gas and oil components of the flow rate, the scope of our modeling included consideration of the reservoir and the natural gas flow rate. While we focused on the coupling of the reservoir to the well, the Nodal Team explored various scenarios of flow in the well and annulus (1).

In order to share with the reader a sense of the time-frame in which the work was carried out and its urgency, we present the model results below in the order we obtained them, from late May to mid- June 2010. This modeling work produced a wide range of possible flow rates and pointed out the main sources of uncertainty while also quantifying the dependencies of the modeled flow rate on various aspects of the conceptual model and model properties. These sensitivities of flow rate to conceptual model and parameter values are roughly valid over the full range of likely conceptual models considered, and thus have value even if the oil flow rate is presently understood to have been at the lower end of the range we estimated in early June 2010. In addition to presenting our early estimate of the range of oil flow rates, we will present and discuss the significant role that natural gas exsolution from the oil plays in controlling flow rates. There had been little concern about the natural gas flow during the

earlier part of the crisis when oil was the main concern, but the gas release is the subject of recent interest (e.g., 2).

Results

With no hard data on constrictions or resistances to flow in either the well or the BOP, we developed a conceptual model that assumes an open well from the reservoir to the bottom of the BOP (Fig. 1a). As such, our conceptual model is highly idealized and tends to produce maximal flow rates of oil and gas. With the conceptual model of Fig. 1a implemented as a two-dimensional cylindrically-symmetric reservoir domain, with one-dimensional flow in the wellbore, and properties implemented into the model as shown in Fig. 1b and as given in Tables 1 and 2, we ran forward transient isothermal simulations of the coupled reservoir-wellbore system. We use the concept of a "fluid-entry interval" to indicate the length over which there is hydrologic coupling between the wellbore and the surrounding reservoir formation. This use of fluid-entry interval is a convenient parameterization of the resistance in the well-reservoir fluid coupling regardless of the actual nature of the coupling (e.g., damaged casing or failed cement job).

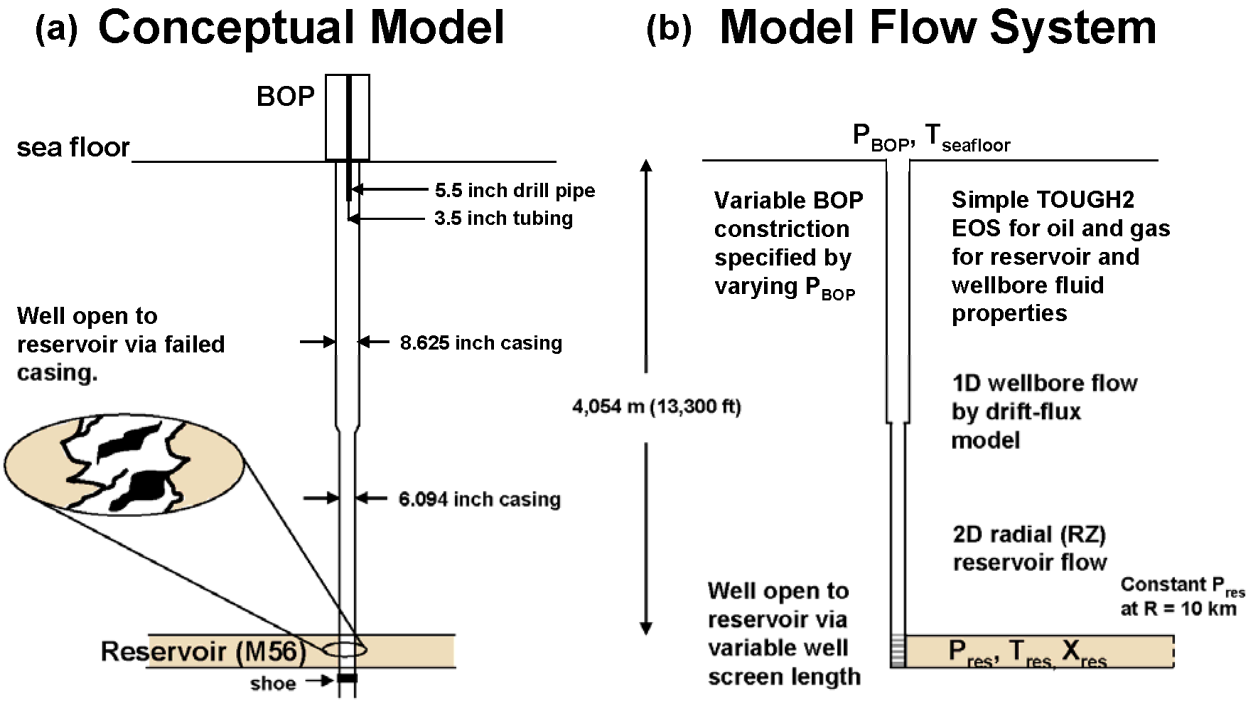

Fig. 1. (a) Conceptual model (not to scale) showing reservoir, well, and blowout preventer (BOP) with potential obstructions (drill pipe, and tubing). (b) Simplified isothermal model system (not to scale) showing reservoir pressure (P_{res}), temperature (T_{res}), and composition (X_{res}), variable fluid-entry interval, well, and top boundary condition representing pressure at the bottom of the BOP (P_{BOP}).

Table 1. Properties of the model system.

Property	Value	Alternate units	Comment or Example Source
Sea Floor Properties			
Temperature at the sea floor	5 °C	41 °F	Approximate value
Depth to the sea floor	1,544 m	5,067 ft	http://www.theoildrum.com/node/6493
Pressure at the sea floor	15.45 MPa	2,241 psia	Calculated assuming average density of sea water is 1020 kg m^{-3}
Well Properties			
Length of 9 7/8 in casing	2,400 m	7,700 ft	Derived from Macondo Well diagram[1]
ID of 9 7/8 in casing	0.22 m	8.6 in	www.jsdrilling.com.qa/Services/Downloads/casing_data.PDF
Length of 7 ½ in casing	1,700 m	5,500 ft	Derived from Macondo Well diagram[1]
ID of 7 ½ in casing	0.15 m	6.1 in	www.jsdrilling.com.qa/Services/Downloads/casing_data.PDF
Roughness coefficient	4.5 x 10^{-5} m	0.18 x 10^{-3} in	Assuming Hazen-Williams coeff. = 100–120
Reservoir Properties			
Depth below sea floor	4,053.8 m	13,300 ft	http://www.theoildrum.com/node/6493
Thickness	30.5 m	100 ft	Approximate value
Porosity	0.22	–	Plume Team PIV report[2]
Permeability	5 x 10^{-13} m^2	0.5 Darcies	Approximate value
Pressure	82 MPa	12,000 psia	Plume Team PIV report[2]
Temperature	130 °C	260 °F	Macondo Well diagram[1]
Fluid Properties			
API Gravity	35 °		Plume Team PIV report[2]
Gas-oil ratio[3]	3,000 scf/STB		Plume Team PIV report[2]
Gas density[3]	0.94 kg m^{-3}		Assumed mixture composition, calculated with WebGasEOS[4]
Gas viscosity[3]	1.5 x 10^{-5} Pa s		Pure methane, calculated with WebGasEOS[4]

[1] http://www.energy.gov/open/documents/3.1_Item_2_Macondo_Well_07_Jun_1900.pdf
[2] Plume Team FRTG (2010) Deepwater Horizon Release Estimate of Rate by PIV, July 21, 2010. http://www.doi.gov/deepwaterhorizon/loader.cfm?csModule=security/getfile&PageID=68011
[3] at standard conditions (1 atm, 60 °F = 0.1013 MPa, 15.5 °C)
[4] http://esdtools.lbl.gov/gaseos/

Because the nature of the opening from the reservoir into the well was unknown, we carried out a series of forward model simulations with varying fluid-entry interval. In our simulations, the oil flow rate became nearly steady by 10 days, the end time for all results shown in this paper. Each simulation required approximately one minute on a single processor of a Linux cluster (Monte Carlo simulations were conducted in parallel on the cluster). As shown in Fig. 2, the near-steady-state oil flow rate after 10 days is a strong

function of fluid-entry interval, varying from about 56,000 bbl/d for a fluid-entry interval of 1.5 m to 100,000 bbl/d for a fluid-entry interval that spans the entire 30-m thickness of the reservoir. Gas flow rate is also shown in Fig. 2 to vary from about 160 MMscf/d to 290 MMscf/d when fluid-entry interval varies from 1.5 m to 30 m. It should be noted that at the time of the MC252-1 blowout, the well had not been intentionally perforated in the reservoir, and the exact pathway by which fluids may have entered the casing was not known.

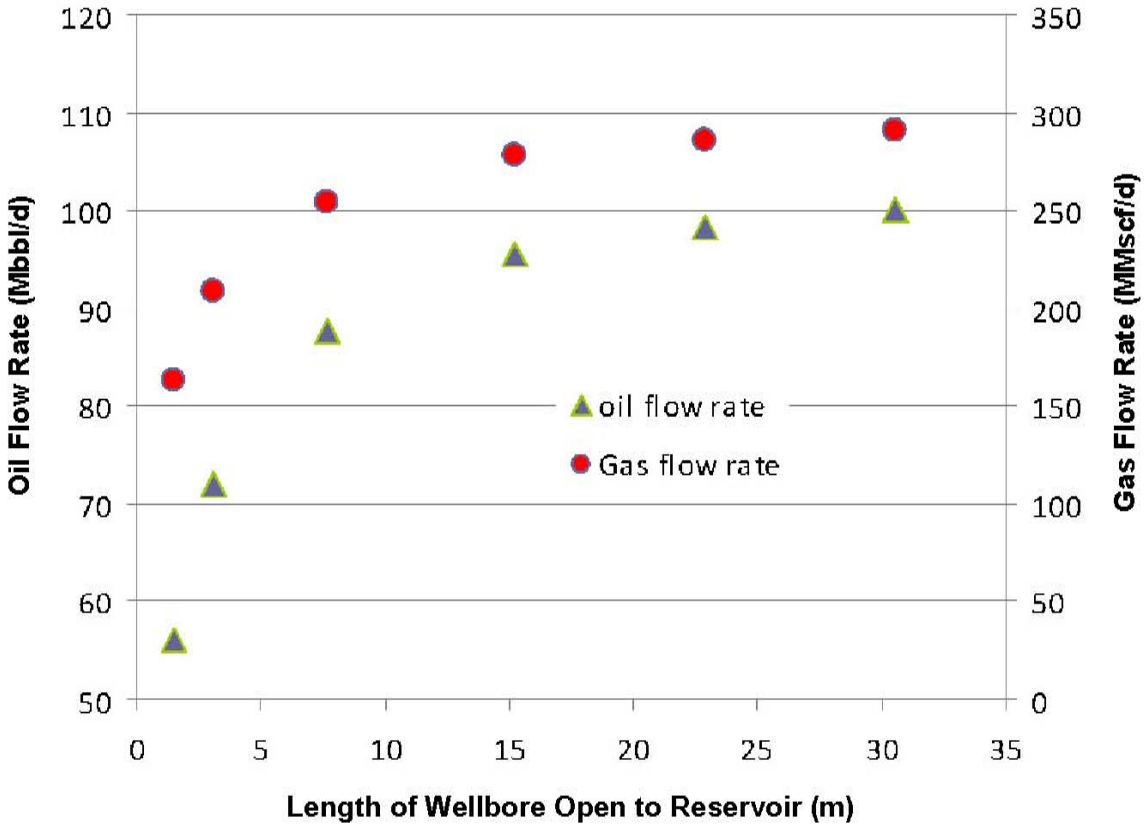

Fig. 2. Results of near-steady-state flow rates for oil (Mbbl/d) and gas (MMscf/d) as a function of fluid-entry interval in the reservoir.

Simulated pressures in the reservoir for a fluid-entry interval spanning the bottom half of the reservoir are shown in Fig. 3 over 5,000 m of radial distance and 5 m of radial distance (inset). The radial extent of the model is 10 km, where a constant-pressure boundary maintains the pressure at its initial value ranging from 81.7 MPa (top of reservoir) to 82.0 MPa (bottom of reservoir). Note this and other reservoirs in the area are overpressured relative to hydrostatic conditions. As shown, pressure gradients are localized around the well and the far-field pressure is not very sensitive to the fluid-entry interval while the near-field pressure is strongly controlled by the fluid-entry interval. These results served to satisfy us that knowledge about the lateral extent of the reservoir was not critical to estimating flow rate as long as the radius was larger than about 1-2 km.

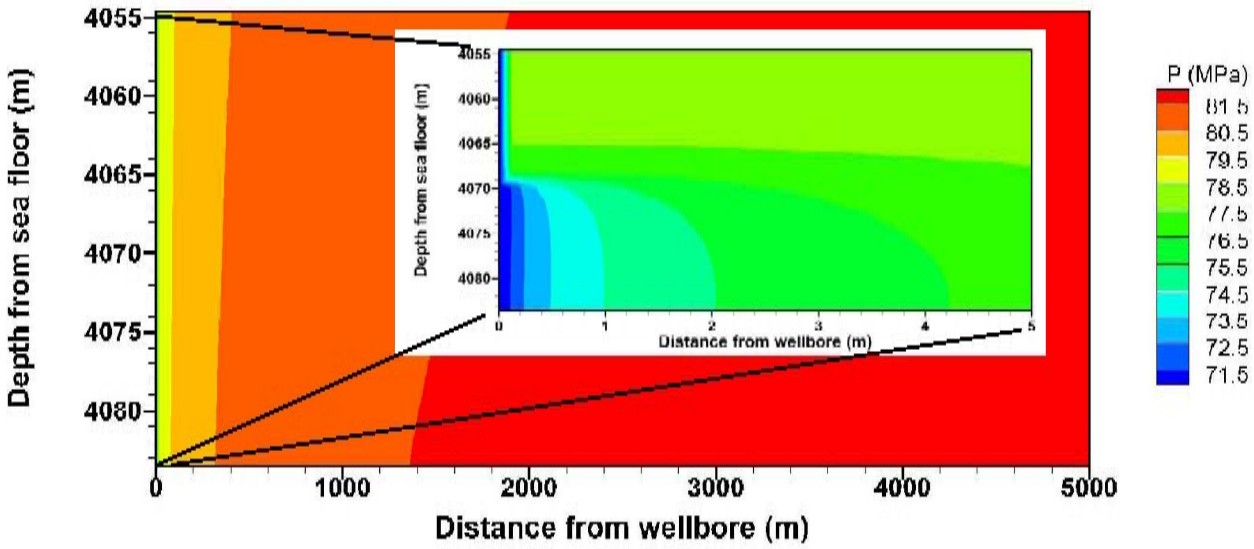

Fig. 3. Variation of reservoir pressure over 5 km of radial distance (distance from wellbore) and 5 m of radial distance (inset) in the reservoir under conditions of flowing oil for fluid-entry interval spanning the lower one-half of the reservoir. Initial reservoir pressure is hydrostatic from 81.7 (top) to 82.0 MPa (bottom).

We varied the main unknown parameters as shown in Table 3 while holding the fluid-entry interval at a value of 30 m (full reservoir thickness), a conservative assumption that will maximize flow rate. Results of 500 Monte Carlo simulations are shown in Fig. 4. The resulting distribution shows the most likely result is 105,000 bbl/d with a long tail extending down to around 65,000 bbl/d. The simulations showed strong sensitivity to reservoir permeability and gas-oil ratio (GOR). We note that our model reservoir is assumed to be 30.5 m thick with uniform permeability across this thickness whereas the actual reservoir likely has intervals of high and low permeability, which would cause the reservoir to appear to have lower effective permeability.

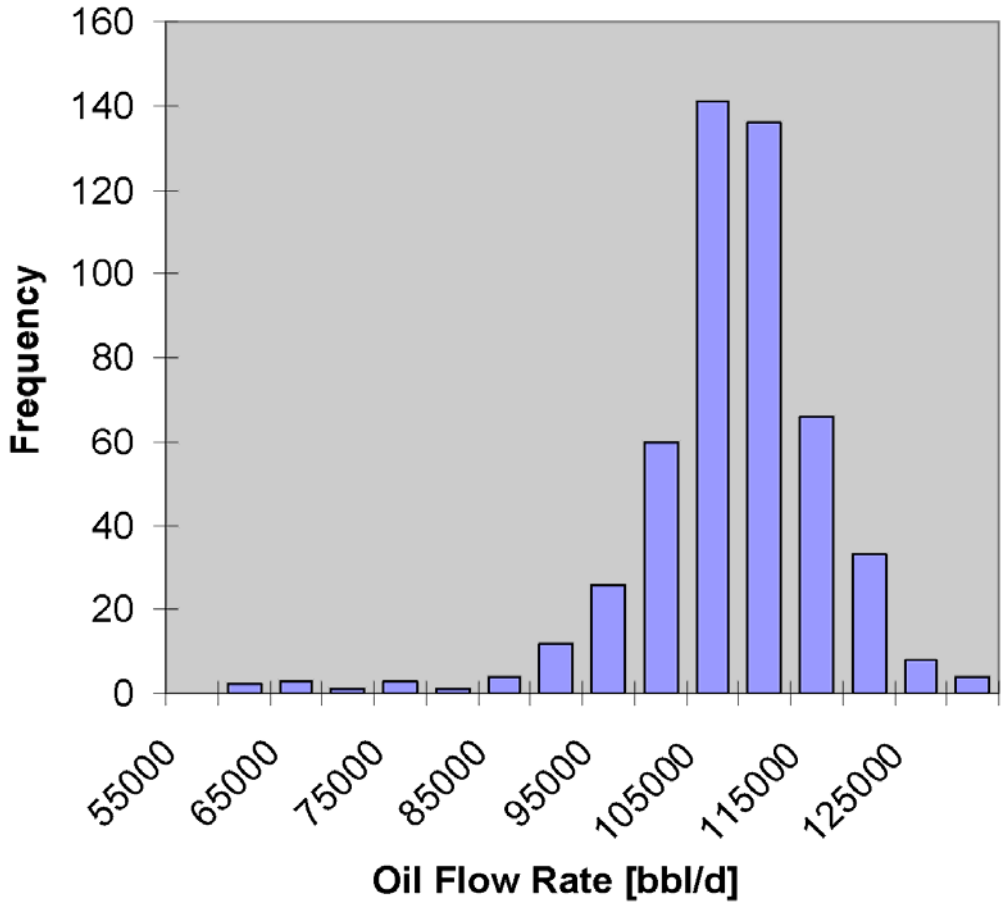

Fig. 4. Results of 500 Monte Carlo simulations with parameter distributions shown in Table 3 showing most likely flow rate of 105,000 bbl/d.

We present in Fig. 5 results of a sensitivity analysis of the oil flow rate as a function of reservoir permeability and GOR. A total of 1,600 forward simulations were carried out to produce the contoured surfaces of oil flow rate. The results of Fig. 5 verify intuition in that high reservoir permeability always increases oil flow rate. Simply put, the more easily the oil flows through the reservoir, the more oil can leak up the well. However, there is more interesting behavior at constant reservoir permeability as a function of GOR, which is the ratio of the volume of free gas that exsolves from a given volume of oil at standard conditions and is most commonly given in units of standard cubic feet per stock-tank barrel (scf/STB). Gas solubility increases with pressure such that oil in the reservoir is single-phase but becomes two-phase as gas exsolves during oil rise and depressurization in the well. Fig. 5 shows that there is a maximum in oil flow rate at a GOR of approximately 1,100 scf/STB for reservoir permeability greater than about 0.2 Darcy (2×10^{-13} m^2). In contrast, the gas flow rate (not shown) monotonically increases with GOR for all permeabilities reflecting the fact that the more gas is present, the more gas can flow up the well. The interesting behavior revealed in Fig. 5 was investigated further as discussed in the next paragraph.

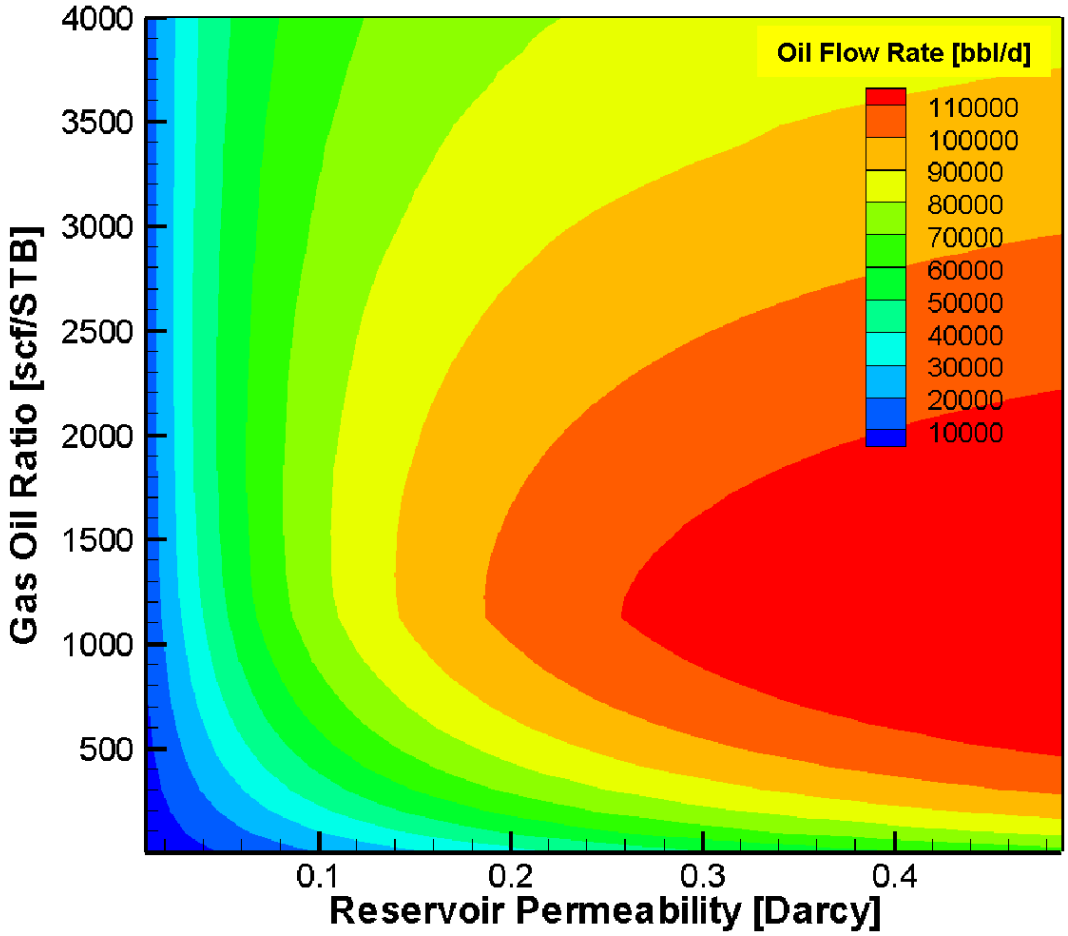

Fig. 5. Oil flow rate as a function of reservoir permeability and gas-oil ratio for P_{BOP} = 4,400 psia (30 MPa).

The unexpected effects of phase interference of gas and oil were revealed by the relatively sophisticated process model we used. The first aspect of the problem that needs to be explained to understand the effect is the role of the top boundary pressure condition. We simplified the unknown flow geometry and resistances of the BOP into a simple pressure boundary condition called P_{BOP}. If P_{BOP} were equal to the pressure at the seafloor, it would imply that the resistances in the BOP are negligible. At the other end of the spectrum, if P_{BOP} were very high, approximately equal to the reservoir pressure minus the pressure due to the hydrostatic column of oil and gas in the well, it would imply the resistance of the flow in the BOP is very large (e.g., rams in the BOP effectively blocking flow). Because the condition of the BOP was not known, we carried out multiple simulations to examine the effect of P_{BOP}. At first glance, it would seem that the main effect of P_{BOP} would be to control the oil flow rate. That is, if the P_{BOP} is nearly equal to the seafloor pressure, the overall driving force for oil from the reservoir would be large and the flow rate correspondingly large. On the other hand, for P_{BOP} equal to P_{res} minus the pressure due to the weight of oil and gas in the well,

there would be no flow at all. However, as suggested by Fig. 5, the situation may not be so simple because of the role of gas exsolution.

We present in Fig. 6 flow rates of dead oil (no gas), and oil (with dissolved gas), along with gas flow rate and gas saturation (fraction of gas phase in the two-phase mixture) as a function of P_{BOP} for GOR = 3000 scf/STB for a fluid-entry interval spanning one-half the reservoir thickness. The gas flow rates are shown for the gas phase itself (free-phase) and for dissolved gas (component). The surprising observation of interest here is the relative lack of dependence of oil flow rate on P_{BOP} until P_{BOP} equals about 6,600 psia (pounds-force per square inch, absolute) (45 MPa), which is the pressure at which no gas exsolves.

There are multiple processes playing off one another in controlling the oil and gas flow rates over the range of P_{BOP} greater than 2,200 psia and less than 6,600 psia (15 MPa < P_{BOP} < 45 MPa). First, the driving force for upward flow in the well decreases for larger P_{BOP}, and second, less gas exsolves for larger P_{BOP}. The effect of less gas exsolution is two-fold: (1) less phase interference results in greater oil flow; and (2) the column contains less gas and therefore exerts a greater hydrostatic pressure against the reservoir. For P_{BOP} less than 6,600 psia (45 MPa), gas exsolves in the well interfering with oil flow while also reducing the weight of the column which tends to enhance the oil flow.

The gas saturation curve in Fig. 6 shows that for P_{BOP} greater than 6,600 psia (45 MPa), no gas exsolves, resulting in the oil flow rate declining sharply because there is less driving force and no gas phase interference. For a hypothetical dead oil (no dissolved gas), the flow rate declines steadily as P_{BOP} increases. In summary, if gas exsolves from the oil, the oil flow rate declines as P_{BOP} increases (less driving force), but this decline is gentle because of the compensating effect of less gas exsolving as P_{BOP} increases. The relative insensitivity of oil flow rate to P_{BOP} was not anticipated, and underscores the importance of modeling coupled processes to capture potential interplay between processes.

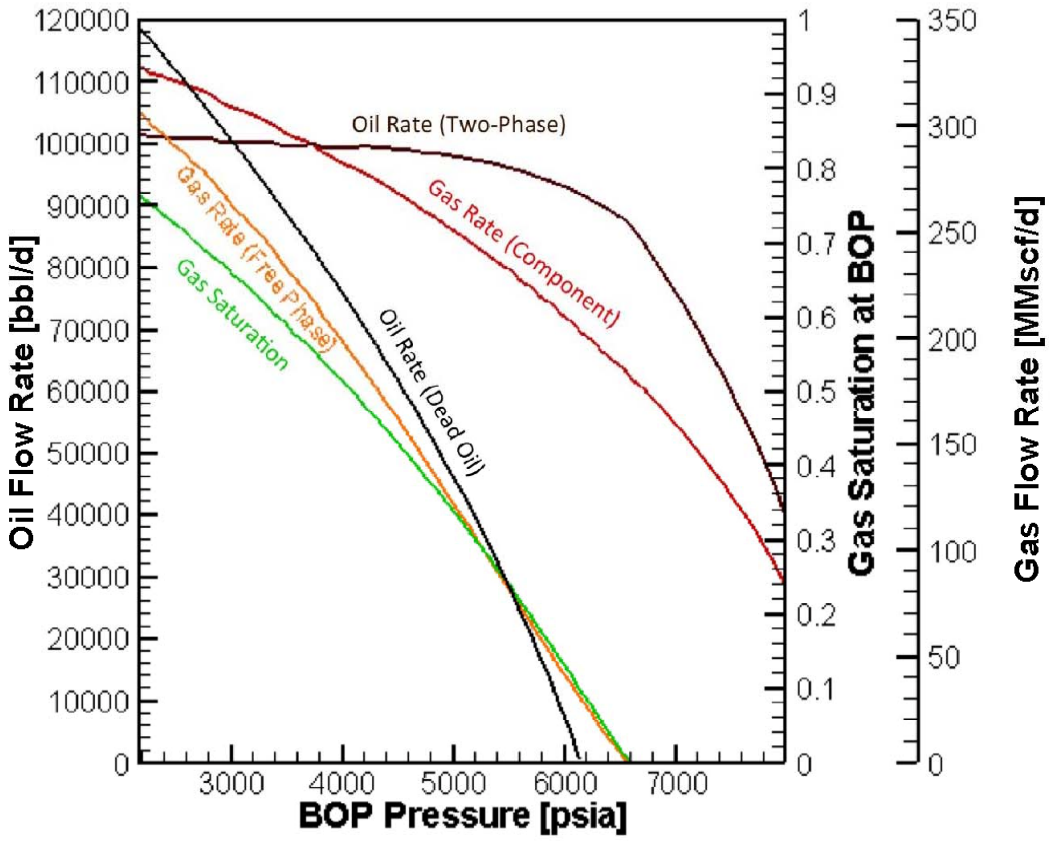

Fig. 6. Oil flow rate, gas saturation, and gas flow rate as a function of P_{BOP}, for GOR = 3,000 scf/STB. The P_{BOP} range shown extends from sea-floor pressure (no flow restrictions in BOP) to an arbitrary pressure equal to 8,000 psia.

Discussion

Our estimates of oil and gas flow rate span a wide range due to multiple uncertainties, most notable of which are length of well open to the reservoir (fluid-entry interval), reservoir permeability, and pressure at the bottom of the BOP. In early August 2010, the final estimates of the larger FRTG from independent analyses and observations were given as 62,200 bbl/d upon initial blowout in April, declining to 52,700 bbl/d just before the well was effectively capped in mid-July. These values are within the range of estimates established by our team as presented above. The decrease in flow rate over time was attributed to pressure depletion in the reservoir as oil and gas leaked out (3). Through comparison of the final independent modeling and observation-based estimates of the FRTG participants, our sensitivity analysis to fluid-entry interval suggested that the well was likely open to the reservoir over only a small interval (1-2 m or so of well-pipe length), or involved fluid entry through a narrow opening , e.g., through a collapsed casing. . Furthermore, the oil flow rate was only weakly controlled by the pressure at the bottom of the BOP due to interplay between P_{BOP} and gas exsolution. Assuming a GOR of 3000 scf/STB, the gas flow rate is estimated at about 160 MMscf/d.

Methods

Data Gathering

Data gathering for conceptual model development was carried out under the pressure of a short deadline for making an estimate of oil flow rate. One of the challenges was that there was no single repository of data available but rather bits of information from various sources. Furthermore, our Nodal Team group was not privy to the proprietary data being shared with other DOE engineers and scientists who were onsite at the Houston facility managing the spill control effort. Through telephone conference calls and emails with National Lab team colleagues, web searching, and the literature, we were able to develop rough estimates of the well, reservoir, and fluid properties.

There were three major gaps in knowledge about the system: (1) the condition of the well and its connectivity to the reservoir; (2) the actual flow path up the well, i.e., whether flow was within the casing or within the annulus or some combination; and (3) the flow path of oil and gas in the BOP. Regarding the first major uncertainty, the well had not been intentionally perforated in the reservoir. This meant that damage to the casing or a failed cement job had led to reservoir fluids entering the well, and the extent and geometry of this reservoir-well connection was unknown except to the extent that significant flow rates of oil and gas were sustained through it. The flow path up the well was also not known, but because the well could clearly sustain significant flow, we assumed the simplest geometry for flow up the well, namely, flow in a round pipe. Similarly, whether or not the various rams in the BOP had deployed and to what extent was unknown except that it was not sealing the well against leakage. The other major data gap was any information about or measurement of pressure of the oil and gas as it leaked out of the riser pipe and later the top of the BOP. We assembled available data on seafloor conditions, well characteristics, reservoir properties, and fluid properties, while leaving the major data gaps as targets of sensitivity studies for the simulations.

Assembling the Model Components

TOUGH2

The computational foundation of our simulation effort was LBNL's non-isothermal, multiphase and multicomponent reservoir simulator TOUGH2 (4,5). TOUGH2 uses an integral finite difference (i.e., finite volume) method to solve a multiphase version of Darcy's Law, with mass and heat transport by advection and diffusion. Implicit time stepping is used along with Newton's method for handling non-linearity within each time step. As long-time developers and users of TOUGH2, we were able to quickly modify the code and adapt useful add-ons developed over the years for other applications to address the urgent need to estimate an oil and gas flow rate. The additions to TOUGH2 and model components that we used for the oil and gas flow rate estimate are described below.

Eoil

The only new code development activity required was development of a new Equation of State (EOS) module for TOUGH2. Given the short time frame, our approach was to approximate oil as a single-component liquid with a dissolved volatile component (natural

gas) that would form a separate phase depending on pressure, temperature, and mass fraction of dissolved gas in the oil phase. The fluid properties that need to be calculated by Eoil are oil density, viscosity, and solubility of natural gas as functions of pressure, temperature, and gas-mixture composition.

A Note on Units

The oil industry developed first in North America and as such a combination of English units and miscellaneous non-metric nomenclature specific to oil and gas properties evolved and remains widely used in the industry worldwide. While metric equivalents are provided where practical, there are some units (e.g., API gravity, Darcy, pounds per square foot, barrels, and standard cubic feet) and nomenclature (e.g., M = one thousand) that we use without conversion because they are widely used and understood in the oil and gas community.

Oil Density

The density of oil without dissolved gas (so-called dead oil) as a function of P and T was modeled in Eoil using standard exponential relations as shown in Table 2. The density of single-phase oil in the reservoir (ρ_{ores}) is assumed to be 970 kg m^{-3}, and the fitting parameters for the relations in Table 2 were chosen to approximate the oil density for the range of conditions at the Macondo well. The model used for density of oil with dissolved gas (so-called live oil) is a simple additive volume relation as shown in Table 2 where X_{gas} is the mass fraction of the gas component dissolved in the oil phase.

Oil Viscosity

Oil viscosity (in cP) was modeled in Eoil using the approach of Beggs and Robinson (7) as a function of temperature (°F), API gravity, and amount of dissolved gas (as given by solution gas-oil ratio (SGOR) = R_s where R_s [=] scf/STB). The relations shown in Table 2 were used with constants derived from limited available data. All of the simulations presented here are for isothermal conditions. This approximation is appropriate for conditions where temperature gradients along the wellbore are obliterated by the rapid and near-steady-state upflow of oil.

Solubility of Natural Gas

The solubility of natural gas in oil is given by SGOR which has units of standard cubic feet per stock-tank barrel (scf/STB). The SGOR is the amount of natural gas contained as a dissolved component in a given volume of oil at any P and T. The variation in gas solubility as a function of pressure and temperature can be approximated by an exponential function with fitting parameters as shown in Table 2.

Gas Properties

To model density and viscosity of the gas phase, we make use of LBNL's WebGasEOS routines (http://esdtools.lbl.gov/gaseos/) (8). We approximate solution gas as pure methane and use the Soave-Redlich-Kwong equation of state to calculate gas density as a function of P and T with a multiplier to adjust to an approximate gas mixture assuming the composition is primarily methane with minor butane, ethane, CO_2, and N_2. Gas viscosity is calculated using the method of Chung et al. (9), assuming the gas is pure CH_4.

Table 2. Fluid property model equations.

Property	Ref./Comment
Density of dead oil[1] (kg m^{-3})	
$\rho_{oild} = \rho_{ores} d_{rel} e^{-a_1(T-a_2)}$ where T is in units of ^{o}C, and P is in Pa and $d_{rel} = b_0 + b_1(e^{-b_2 P/10^6})$	(6)
Density of live oil[2](kg m^{-3})	
$\frac{1}{\rho_{oil}} = \frac{(1-X_{gas})}{\rho_{oild}} + \frac{X_{gas}}{\rho_{gas}}$	Simple mixing relation.
Viscosity of dead oil (cP, °F, API)	
$\mu_d = 10^{x-1}$ where $x = 10^{\frac{(a_1 - a_2 \times API)}{T^{a_3}}}$	(7)
Viscosity of live oil (cP, °F, scf/STB)	
$\mu_{bubble} = a\mu_d^b$ where $a = \frac{a_1}{(R_s+100)^{a_2}}$, $b = \frac{b_1}{(R_s+150)^{b_2}}$,	(7)
Gas solubility, SGOR (scf/STB, psia, °F)	
$R_s = R_{s0} + A \times P^B$, $R_{s0} = -r_1 + r_2 e^{(-r_3 T)}$ $A = a_1 + a_2 e^{(-a_3 T)}$, $B = b_1 - b_2 e^{(-b_3 T)}$	Assumed exponential relation.

[1]Dead oil refers to oil without dissolved gas.
[2]Live oil refers to oil with dissolved gas.

T2Well

While the foundation of the simulation effort described here is TOUGH2, the key process model component that sets this effort apart from the work of other groups in the FRTG is T2Well (10), which provides wellbore flow simulation capabilities for TOUGH2. With T2Well, all of the reservoir simulation capabilities of TOUGH2 are coupled to a one-dimensional drift-flux model for wellbore flow. This capability was originally developed for geologic carbon dioxide sequestration studies, with the fluid components being CO_2 and saline water, but T2Well can be used with any two-phase TOUGH2 EOS module. Once Eoil was completed, we coupled it with T2Well and ran the fully coupled flow of oil and gas in the reservoir and into and up the wellbore to the top of the system at the bottom of the BOP.

iTOUGH2

Rounding out the simulation components we used for estimating the oil and gas flow rate is the iTOUGH2 code with uncertainty and sensitivity analysis capabilities (11,12). Briefly, iTOUGH2 is a wrapper around the codes described above that calls the forward model repeatedly while varying key input parameters to produce multiple results as a function of input parameter variations. We used iTOUGH2 in two modes in the analysis: (1) to calculate local and global sensitivities to input parameters, and (2) to carry out Monte Carlo simulations for quantifying the uncertainty in the predicted flow rate. Insights on global sensitivities were gained by evaluating simulation results for many parameter combinations

over selected cross-sections in the parameter space. The Monte Carlo simulations are done assuming various distributions for the uncertain parameters (see Table 3) and carrying out multiple simulations using random combinations of these parameters. The results allow quantification of the uncertainty in the model predictions. With several poorly constrained parameters and uncertain conceptual model elements, we varied properties of the reservoir, well, and fluids to quantify the uncertainty in our predictions as described in *Results*.

Table 3. Uncertain parameters and distributions for uncertainty quantification.

Parameter	Mean	Range	Standard Deviation
Permeability (k)	4.87×10^{-13} m^2	4.87×10^{-14} – 4.87×10^{-12} m^2	2.44×10^{-13} m^2
Porosity (ϕ)	0.22	0.2 – 0.25	0.03
Pressure in the reservoir (P_{res})	81.7 MPa	81.2 – 82.2 MPa	2.0×10^5 Pa
Temperature in the reservoir (T_{res})	128 °C	118 – 138 °C	5 °C
Gas-Oil Ratio (GOR) at standard T and P	3,000 scf/STB	1,000 – 4,000 scf/STB	500 scf/STB
Gas density at standard T and P (GST)	0.980 kg/m^3	0.948 – 0.991 kg/m^3	0.01 kg/m^3
API Gravity	35°	34° – 39°	1°
Pressure at the bottom of the BOP (P_{BOP})	22 MPa (3,190 psia)	19 – 25 MPa (2,755 – 3,625 psia)[1]	1 MPa (145 psia)

[1]Plateau region of Fig. 6.

Acknowledgments

We thank George Guthrie and Grant Bromhal (NETL) for leadership and organization of the Nodal Team, and Maria Barrufet (Texas A&M University) for advice on fluid property models. We also thank Christine Doughty (LBNL) and two anonymous reviewers for detailed review comments and helpful suggestions on earlier drafts. This work was supported by a Work for Others agreement through the National Energy Technology Laboratory, of the U.S. Department of Energy under Contract No. IW007439; and by the Assistant Secretary for Fossil Energy, Office of Natural Gas and Petroleum Technology, of the U.S. Department of Energy under Contract No. DE-AC02-05CH11231.

Abbreviations, Units, and Nomenclature

API gravity	American Petroleum Institute measure of density of oil
bbl	Barrel (42 gallons, or 0.16 m^3)
cP	Centipoise (10^{-3} Pa s)
BOP	Blow out preventer
Darcy	Measure of permeability (10^{-12} m^2)
DOE	U.S. Department of Energy
GOR	Gas-oil ratio (volumetric ratio of free gas to oil at 1 atm, 60 °F**)**
LANL	Los Alamos National Laboratory
LBNL	Lawrence Berkeley National Laboratory
LLNL	Lawrence Livermore National Laboratory
M	one thousand
MMscf	Million standard cubic feet (2.83×10^4 m^3)
NETL	National Energy Technology Laboratory
PIV	Particle Image Velocimetry
PNNL	Pacific Northwest National Laboratory
Riser	Pipe connecting wellhead/BOP with platform
Scf	Standard cubic foot (at 1 atm, 60 °F (0.1012 MPa, 15.5 °C)
SGOR	Solution gas-oil ratio (solubility of natural gas in oil)
STB	Stock Tank Barrel (one barrel of dead oil at standard conditions)
UQ	Uncertainty quantification

Property Variables

μ_d	Viscosity of dead oil (cP)
μ_{bubble}	Viscosity of oil at the bubble point (cP)
P	Pressure (MPa)
ρ_{gas}	Density of gas (kg m^{-3})
ρ_{ores}	Density of oil in the reservoir (kg m^{-3})
ρ_{oil}	Density of oil (kg m^{-3})
ρ_{oild}	Density of dead oil (kg m^{-3})
R_s	Solubility of gas in oil, aka SGOR (scf/STB)
T	Temperature (°F or °C)
X_{gas}	Mass fraction of gas in the oil (-)

References

1. McNutt M, Camilli R, Guthrie G, Hsieh P, Labson V, Lehr B, Maclay D, Ratzel A, Sogge M (2011) Assessment of flow rate estimates for the Deepwater Horizon /Macondo Well oil spill. *Flow Rate Technical Group report to the National Incident Command*, Appendix F,, Interagency Solutions Group, U.S. Department of the Interior, Washington, DC, March 10, 2011.

2. Joye SB, MacDonald IR, Leifer I, Apser V (2011) Magnitude and oxidation potential of hydrocarbon gases released from the BP oil well blowout, *Nature Geoscience, 4*:160-164.

3. Hsieh P (2010) Computer simulation of reservoir depletion and oil flow from the Macondo well following the Deepwater Horizon blowout: *U.S. Geological Survey Open-File Report 2010–1266*, 18 pp, U.S. Geological Survey, Reston VA.

4. Pruess K, Oldenburg CM, Moridis GJ (1999) TOUGH2 User's Guide Version 2. E. O. Lawrence Berkeley National Laboratory Report *LBNL-43134*, Lawrence Berkeley National Laboratory, Berkeley CA.

5. Pruess K (2004) The TOUGH Codes—A Family of Simulation Tools for Multiphase Flow and Transport Processes in Permeable Media, *Vadose Zone J., 3*, 738 - 746.

6. Aziz K, Settari A (1985) *Petroleum Reservoir Engineering* (Elsevier, New York) 476 pp.

7. Beggs HD, Robinson JR (1975) Estimating the viscosity of crude oil systems, *J. Pet. Tech.* (Sep.), *27*:1140–1141.

8. Reagan MT, Oldenburg CM (2006) WebGasEOS v1.0 User Guide, Lawrence Berkeley National Laboratory Report *LBNL-3188*, Lawrence Berkeley National Laboratory, Berkeley CA.

9. Chung TH., Ajlan M, Lee LL, Starling KE (1988) Generalized multiparameter correlation for nonpolar and polar fluid transport properties, *Ind. Eng. Chem. Res., 27*(4), 671–679.

10. Pan L, Oldenburg CM, Wu YS, Pruess K (2011) T2Well/ECO2N Version 1.0: Multiphase and Non-Isothermal Model for Coupled Wellbore-Reservoir Flow of Carbon Dioxide and Variable Salinity Water, Lawrence Berkeley National Laboratory Report *LBNL-4291E*, Lawrence Berkeley National Laboratory, Berkeley CA.

11. Finsterle S (2004) Multiphase inverse modeling: Review and iTOUGH2 applications, *Vadose Zone J.*, 3: 747–762.

12. Finsterle S, Zhang Y (2011) Solving Simulation-Optimization Problems using iTOUGH2 with the PEST Protocol, *Environmental Modelling and Software, 26*:959-968.

DISCLAIMER